Fat- and susceptibility-corrected R2* mapping for liver iron quantification: preliminary evaluation in a healthy cohort

Diego Hernando[1], Jens-Peter Kühn[1,2], and Scott B Reeder[1,3]

[1]*Department of Radiology, University of Wisconsin-Madison, Madison, WI, United States,* [2]*Department of Diagnostic Radiology, University Greifswald, Greifswald, MV, Germany,* [3]*Department of Medical Physics, University of Wisconsin-Madison, Madison, WI, United States*

Introduction: MRI is very sensitive to the presence of iron, and can be used to assess body iron deposition for diagnosis, staging and treatment monitoring of iron overload [1]. R2*-MRI (quantification of R2* relaxivity from a sequence of gradient echo images with increasing echo times) correlates well with liver iron content [1]. Unfortunately, R2* is affected by confounding factors, including fat [2], noise floor and susceptibility effects [3]. Recently, a method was introduced for correcting these confounding factors by performing fat-corrected (to remove R2* errors due to the presence of fat), complex-fitting (to avoid the noise floor), and susceptibility-corrected (to remove R2* errors in regions of rapid Bo field variation) R2* mapping. Susceptibility correction is performed by measuring the Bo field from the complex data itself, and correcting for the effect of field variations within each voxel [4]. In this work, we evaluate the susceptibility correction in a cohort of 35 healthy subjects without iron overload.

Materials and Methods: Upon IRB approval, liver scans from 35 healthy subjects were obtained at 1.5T using a 3D multi-echo spoiled gradient echo sequence [5], with 6 TEs (TE_1=1.2ms, ΔTE=2.0ms), flip angle=5°, slice thickness=10mm, and 32 slices. Each subject was scanned twice to test measurement repeatability. Data from one subject were discarded due to severe motion artifacts. Fat-corrected, susceptibility-uncorrected R2* maps were reconstructed offline using a fat-water separation algorithm including multi-peak fat modeling and R2* estimation [2]. Fat- and susceptibility-corrected R2* maps were obtained as described in Ref. [4]. Note that susceptibility correction is performed from 3D measurements accounting for the acquisition (3D Cartesian) and reconstruction (*k*-space windowing using a modified Tukey filter [6]), both of which affect the distribution of resonances contributing to the signal at an individual voxel in the presence of macroscopic field variation. Measurements (ROIs) were taken by one radiologist with >5 years of experience in liver imaging. ROIs were measured from all 9 Couinaud segments, plus a volumetric measurement from the complete liver.

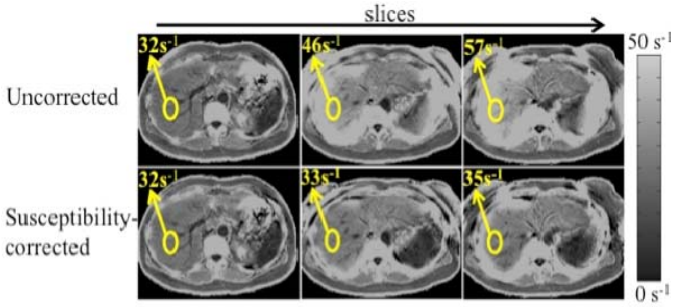

Figure 1. Representative liver R2* results in a healthy volunteer, in several slices approaching the liver dome.

Results: Data from one patient were discarded due to severe motion artifacts. In one patient, a giant hemangioma in the right lobe precluded measurement of R2* in segment 7, as well as a whole liver R2* measurement. Measurements from the other 8 segments were included. Figure 1 shows a representative example of susceptibility-uncorrected and corrected reconstructions in a healthy subject. Figure 2 shows measurements over all subjects and all Couinaud segments, as well as volumetric (whole-liver) measurements. The mean R2* measurement over all subjects and all segments was 35.8 (uncorrected) and 33.3 (corrected), both in good agreement with literature values [7]. However, uncorrected measurements were highly elevated in segments near the dome of the liver, particularly segments 4a, 7 and 8. These findings agree with the Bo field gradients measured in these segments (Figure 3). In segment 8, uncorrected R2* values are often above the pathologic threshold (52 s^{-1}) [8], and may lead to misdiagnosis: in exams where segment 1 (where susceptibility effects are minor) showed R2*<52s^{-1}: 29% of uncorrected R2* in segment 8 had R2* above the threshold, compared to 0% for corrected measurements. From the repeatability tests, the 95% limits of agreement for uncorrected and corrected measurements were 0.53±10.89 and -0.19±8.83, respectively, demonstrating that susceptibility correction improves precision of R2*-MRI.

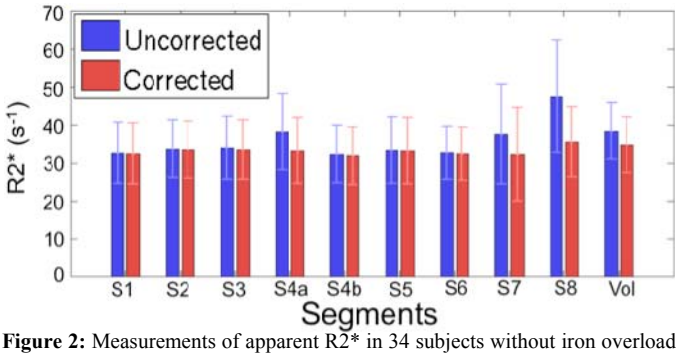

Figure 2: Measurements of apparent R2* in 34 subjects without iron overload without (blue) and with (red) susceptibility correction. The uncorrected R2* measurements appear elevated in segments 4a, 7 and 8. The corrected R2* measurements are more homogeneous for all segments.

Discussion: The proposed method produces more homogeneous R2* measurements in healthy subjects without iron overload. In this work, problematic segments were 4a, 7, and 8. However, this may be dependent on the specific liver anatomy in healthy and diseased livers, particularly after liver transplant or partial resection where the anatomy is distorted. Although repeatability improves with susceptibility correction, optimized acquisition parameters (eg. longer echo trains) may lead to further improvements in the precision of R2* measurements. Because rapid field variations appear primarily in the z-direction, it may be advantageous to avoid axial acquisitions where the largest dimension of the voxel is acquired in the z-direction. Susceptibility correction may be important for R2* measurement for liver iron quantification, particularly if localized iron deposition is assessed in regions near the dome of the liver.

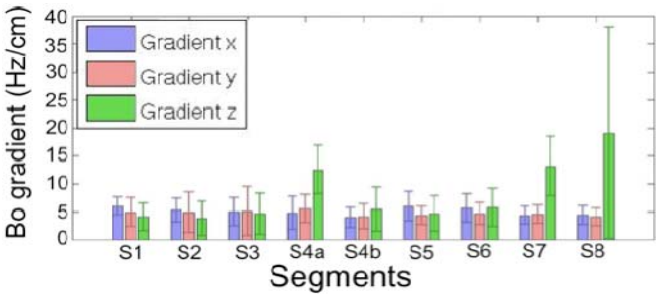

Figure 3: The 3 components of the spatial gradient of the Bo field map measured in all 9 liver segments. The Bo field varies slowly (mean < 7 Hz/cm) for all segments, except those near the dome of the liver (4a, 7 and 8), where it changes rapidly (mean 13, 13 19 Hz/cm respectively) along z.

References: [1] Wood JC, et al, Blood 2005;106:1460-1465. [2] Yu et al, MRM 2008;60:1122–1134. [3] Fernandez-Seara et al, MRM 2000;44:358-366. [4] Hernando D, et al, MRM 2011 (In press). [5] Hines CDG et al, JMRI 2009;30:1215-1222. [6] Polzin JA, et al, RSNA 2003, p. 702. [7] Schwenzer NF, et al, Invest Radiol 2008;43:330-337. [8] Westwood MA, et al, JMRI 2003.

Acknowledgements: We acknowledge the support of the NIH (R01 DK083380, R01 DK088925 and RC1 EB010384), the Coulter Foundation, WARF Accelerator Program and GE Healthcare.